Available online at www.sciencedirect.com
SCIENCE DIRECT®
Sensors and Actuators A 105 (2003) 1–9
SENSORS AND ACTUATORS A PHYSICAL
www.elsevier.com/locate/sna

A rib-reinforced micro torsional mirror driven by electrostatic torque generators

Hung-Yi Lin, Weileun Fang*

Power Mechanical Engineering Department, National Tsing Hua University, Hsinchu 30043, Taiwan

Received 28 March 2002; received in revised form 24 November 2002; accepted 24 December 2002

Abstract

A novel micromachined torsional mirror for use as an optical scanner is reported in this study. The proposed micromachined torsional mirror exploits novel electrostatic actuators and a reinforced thin-film mirror plate to improve the performance of the device. The electrostatic actuator is actuated by near gap-closing electrodes so as to decrease the driving voltage. Moreover, the actuator employs a lever mechanism to magnify its output displacement. A torque generator is implemented by combining two electrostatic actuators, which prevents the mirror plate from wobbling. A reinforced rib is used to stiffen the thin-film mirror plate to improve the optical performance of the scanner. In order to demonstrate the proposed concept, micromachined torsional mirrors were fabricated through the integration of DRIE, surface, and bulk micromachining processes. Measurements revealed that the proposed torsional mirror could operate at a low driving voltage, the scanning frequency of the mirror can reach 17.7 kHz, and the optical scan angle is 5°.
© 2003 Elsevier Science B.V. All rights reserved.

Keywords: Micro torsional mirror; Lever mechanism; Rib-reinforced structure

1. Introduction

Electrostatically driven micro torsional mirrors have been studied extensively since being proposed by Petersen in early 1980 [1]. In Petersen's design, a plate served both as an optical surface and a driving electrode; thus the scanning angle and the size of the plate were restricted by driving-voltage limitations. This kind of torsional scanner is more appropriate in applications using a small-pixel, array-type device such as the DMD [2]. However, there are various applications such as barcode readers [3], laser printers [4], and display [5], requiring a single mirror of dimensions of several hundred microns with a larger scanning angle. The so-called pop-up mirror driven by a comb actuator has been proposed for such applications [3], in which the mirror plate is attached to the substrate via micro hinges [6] so as to produce a larger scanning angle. However, in actual implementations it was found that the supporting structure of the pop-up mirror was not stiff enough to tolerate the distributed inertia forces associated with accelerations during scanning [7], which resulted in divergence of the reflected laser beam and consequently significantly degraded optical resolution. Moreover, the scanning frequency of the mirror plate has to be several tens of kilohertz to reach the required resolution of VGA quality for the application of raster scanning display [7], whereas the line-scan rate of the existing micro torsional mirrors was only several kilohertz. In short, several aspects of the performance of existing scanning mirrors—including mirror flatness, dynamic deformation, driving voltage, and scanning frequency—need to be improved before they can be used in many applications.

This study investigated a novel micro torsional mirror. As shown in Fig. 1a, the torsional mirror contains a stiff mirror plate and a special driving mechanism. Several design issues regarding the stiffness of the mirror plate, the resonant frequencies of the mirror, the angular deflection, and the driving voltage are described here. Briefly, the proposed torsional mirror is intended to have both a larger angular deflection and larger plate size, yet maintain operation at frequencies above 15 kHz. This paper also describes the novel micromachining processes developed to fabricate the torsional mirror.

2. Design issues

Fig. 1a shows the three innovations in the proposed micromachined torsional mirror. Firstly, a novel electrostatic actuator as well as a torque generator was exploited to drive the scanning mirror—the cross-sectional view of the torque

* Corresponding author. Tel.: +886-3-574-2923; fax: +886-3-572-2840.
E-mail address: fang@pme.nthu.edu.tw (W. Fang).

0924-4247/03/$ – see front matter © 2003 Elsevier Science B.V. All rights reserved.
doi:10.1016/S0924-4247(03)00056-6

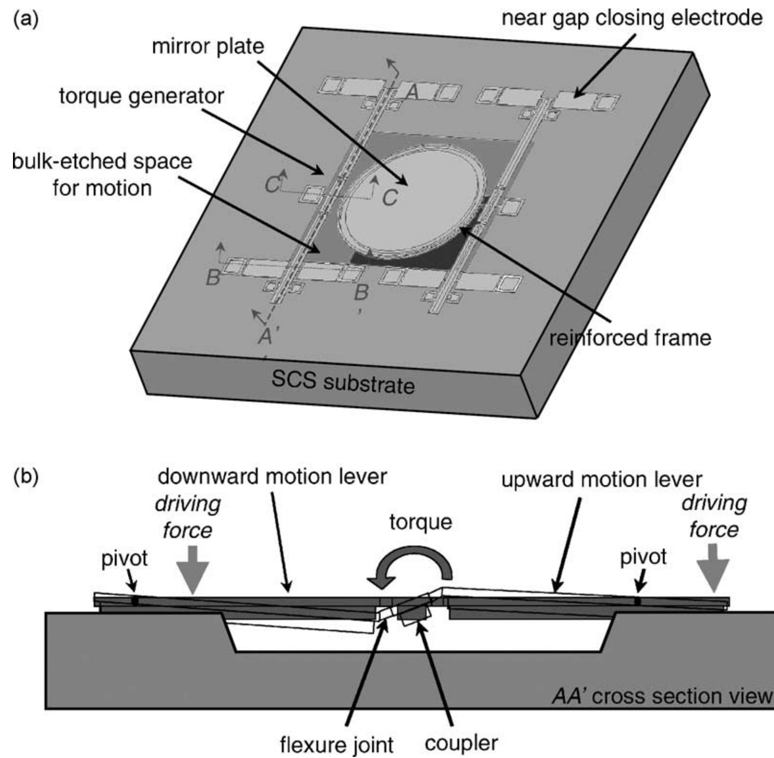

Fig. 1. (a) Schematic plot of the proposed micro torsional mirror, and (b) the AA′ cross-section view (cross-sections BB and CC are referred to in Fig. 7).

generator is provided in Fig. 1b. Secondly, a reinforced frame was designed to increase the stiffness and flatness of the mirror. Thirdly, a three-mass system formed by the mirror and the coupler was developed to increase the resonant frequencies of the scanning mirror device.

2.1. Actuation consideration

The trade-off between traveling distance and driving voltage is a primary consideration when designing an electrostatic actuator. In general, a larger gap between the electrodes increases the traveling distance, but this results in a higher voltage being required to drive the actuator. This work proposes a novel electrostatic actuator to reduce the driving voltage yet increase the angular displacement of the mirror plate.

2.1.1. Leverage electrostatic actuator

As indicated in Fig. 2a, the proposed leverage electrostatic actuator consists of a reinforced lever mechanism and gap-closing parallel-plate electrodes. The driving voltage is low since the gap between the parallel-plate electrodes is small (2 μm). The lever mechanism is employed to amplify the traveling distance of the actuator in the out-of-plane direction [8]. Fig. 2b shows that the lever mechanism contains one arm of length $L\ (= L1+L2)$ and torsional hinges to produce the pivoting motion. If the lever arm is assumed to be a rigid body, the amplification ratio of the lever mechanism is $L2/L1$. However, the low inherent rigidity of a flat thin-film structure places doubt on the assumption of rigid-body motion, and so the loading deformation of the lever arm itself could significantly decrease the ideal amplification ratio of the mechanism.

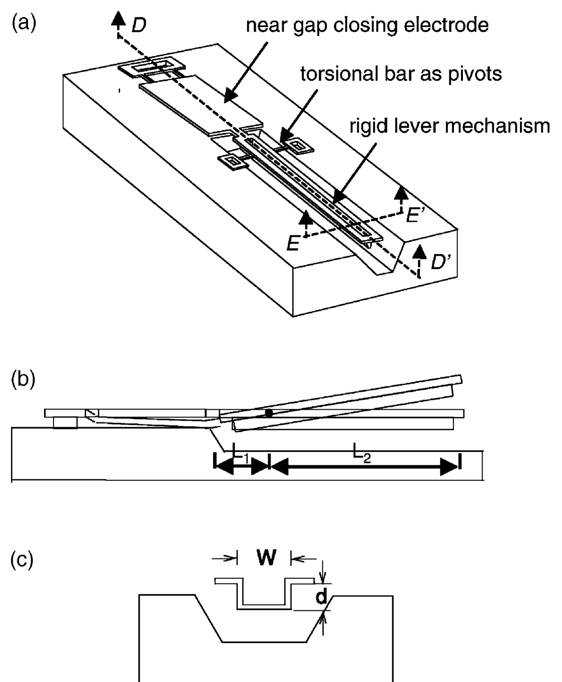

Fig. 2. (a) Schematic plot of leverage electrostatic actuator, (b) the DD′ cross-section view, and (c) the EE′ cross-section view.

The rigidity of the mechanism was increased by fabricating rib-reinforced lever arms using a trench refilled fabrication method [9]—the bending stiffness of the lever arm could be increased by changing the parameters w and d indicated in Fig. 2c. A structural analysis revealed that the 2.5-μm-thick rib-reinforced lever was more than 100-fold stiffer than the conventional one made from the same material when $d = 15\,\mu m$ [9], thereby improving the effective motion amplification by the lever mechanism.

2.1.2. Electrostatic torque generator

The electrostatic electrode is used to generate attractive rather than repulsive force. For a conventional parallel-plate actuator, the suspended upper electrode could only move toward the downward electrode on the substrate surface. Such a driving actuator gives the torsional beam not only a twisting moment but also a transverse load. Consequently, the mirror will experience both rotation and translation. Translatory motion (or "wobble") of the mirror would affect the ability to control the position of the reflected laser beam.

To prevent the mirror from wobbling, this study exploited a novel mechanism to balance the transverse loads on the torsional beam. As indicated in Fig. 1b, a mechanism named a "torque generator" is realized by integrating downward- and upward-motion levers. Both levers are connected to a coupler through flexible joints, and the moving direction of the lever mechanism is determined by the position of the pivot. Thus, this driving mechanism applies only a torque to the mirror plate through the coupler when the levers are driven by the electrostatic force simultaneously. Moreover, since the cross-section of the flexible joint shown in Fig. 1b is not rib reinforced, its stiffness is much smaller than that of the lever arm. As a result, the compliance of the flexible joint allows the coupler to rotate significantly, allowing the mirror to exhibit a larger scanning angle.

2.2. Optical considerations

The optical quality and resolution of the light beam reflected from the torsional mirror depends on the flatness of the mirror plate [5], since deformation of the mirror plate could cause in wavefront distortion. In general, the gradient residual stress will induce a static load that deforms the mirror plate, and the inertial force will induce a dynamic load that distorts the mirror plate when operating at high frequencies. The static deformations of the mirror could be compensated if the curvature of the deformed plate is uniform and the radius of curvature ρ of the deformed mirror is known in advance. However, the curvature of the deformed micro mirror induced by dynamic loads varies with the angular position, and cannot be compensated. Therefore, the plate needs to be as rigid as possible.

According to the Rayleigh criterion [10], the peak-to-valley distortion of the mirror must be less than $\lambda/4$ (where λ is the wavelength of incident light) to prevent significant degrading of the image quality. This corresponds to a required accuracy on the order of 100 nm, which is difficult to achieve for a thin-film mirror plate.

2.2.1. Reinforced thin-film mirror

As illustrated in Fig. 1, a reinforced frame is designed to increase the stiffness of the thin-film mirror plate to improve its optical performance [11]. The outside boundary condition of the mirror plate is changed from a free end to a fixed end. As indicated in Fig. 3, the mirror plate has a reinforced frame with depth d and width w, and the outside diameter and the clear aperture of the mirror are $2R_o$ and $2R$, respectively. There are two advantages of this design: (1) it is still a thin-film structure and hence will not increase the weight of the mirror plate significantly, and (2) it can be fabricated by the trench-refilled process.

The deformation of the mirror due to the dynamic load was investigated analytically. The distributed inertia force deforming the mirror plate is illustrated in Fig. 4. According to a simplified one-dimensional model, the deflection amplitude δ_d of a rectangular mirror plate due to the dynamic response is expressed as [1]

$$\delta_d = 0.226(1-\nu^2)\frac{\mu L^5}{Et^2}(2\alpha\omega^2) \tag{1}$$

where L represents the length of the plate, ω and α represents the scanning frequency and angle, respectively, and μ represents the density of the thin-film material. Eq. (1) indicates that the deformation of the mirror plate due to dynamic loads becomes an important issue for a large-aperture mirror operated at high frequencies and/or a large scan angle.

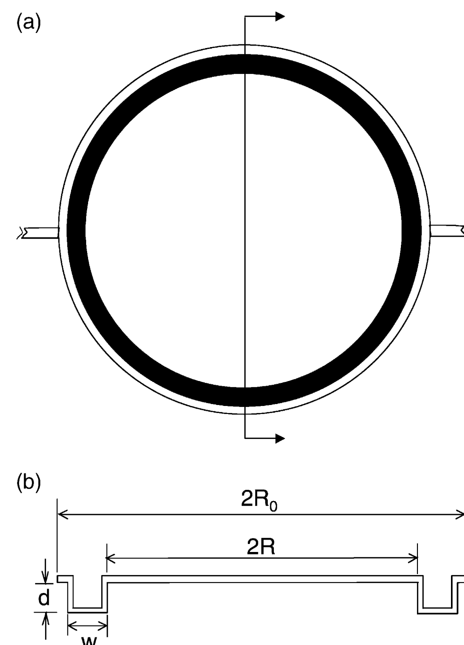

Fig. 3. The proposed mirror plate reinforced by a folded frame (a) top view, and (b) cross-section view.

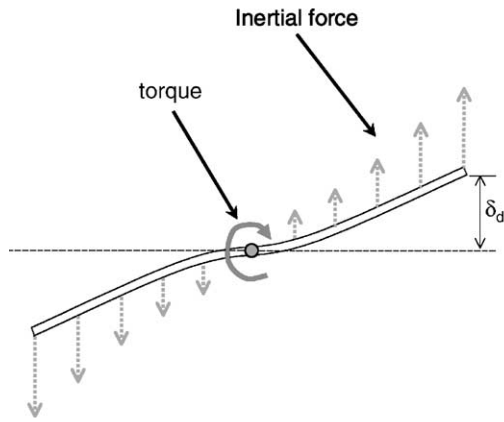

Fig. 4. The dynamic distributed loads applied on the mirror plate.

A three-dimensional finite element model was also established to analyze the deformation of the circular mirror plate during scanning. The model contained mirror plate (with $R = 275\,\mu$m) subjected to a distributed inertia force. The inertia force is determined from the size of the mirror plate, the scanning frequency ω, and the scanning angle α. The deformation of the mirror plate analyzed through the FEM model is shown in Fig. 5a. The maximum deformation was $0.74\,\mu$m in the half span of the mirror, when the mirror plate was operating at $\omega = 15\,$kHz [1] and $\alpha = \pm 5^\circ$. Fig. 5b shows the deformation of the mirror plate with a folded frame as in Fig. 3. The maximum deformation is reduced 5.5-fold to $0.135\,\mu$m in the half span under the same operating conditions, indicating that the proposed structure also significantly improves the flatness of the mirror plate during scanning.

The analysis also demonstrated that the use of the proposed reinforced frame the mass of the mirror plate with $d = 15\,\mu$m and $w = 20\,\mu$m only 1.5-fold over that of a conventional plate with the same clear aperture R. Further, the deviation between the axis of rotation and the center of gravity of the plate with the folded frame is less than 0.01%. Consequently, the excitation due to the unbalanced rotating mass can be ignored and hence wobble motion is prevented.

2.3. Vibration modes

The torsional mirror is designed to have a large scanning angle and high scanning frequency to increase its resolution. The torsional mirror is usually driven at its resonant frequency to increase the scanning angle, and in order to meet the resolution requirements of VGA monitors, the mirror needs to have a scanning rate higher than 15 kHz. In other words, the scanner should have it torsional vibration mode higher than 15 kHz. However, it is difficult for the existing micromachined scanner to achieve.

This study proposes a scanner with various torsional vibration modes. As illustrated in Fig. 1, the mirror plate and the couplers can be regarded as a three-mass system, which

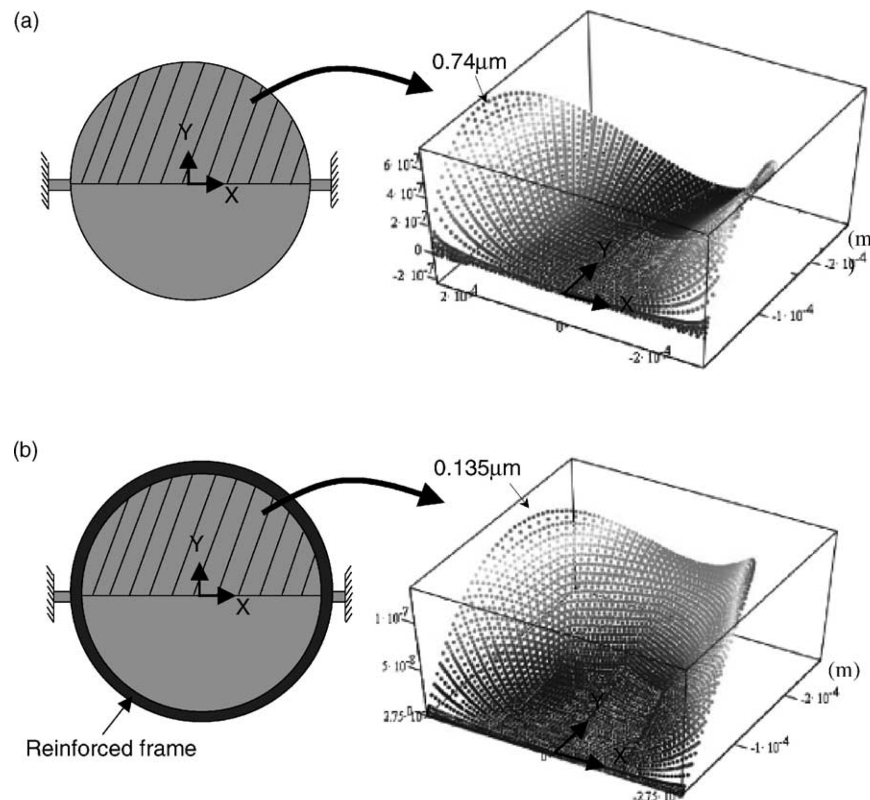

Fig. 5. The simulation results of mirror plates (half span) deformed by dynamic loading for (a) the mirror plates without folded frame, and (b) the mirror plate with folded frame.

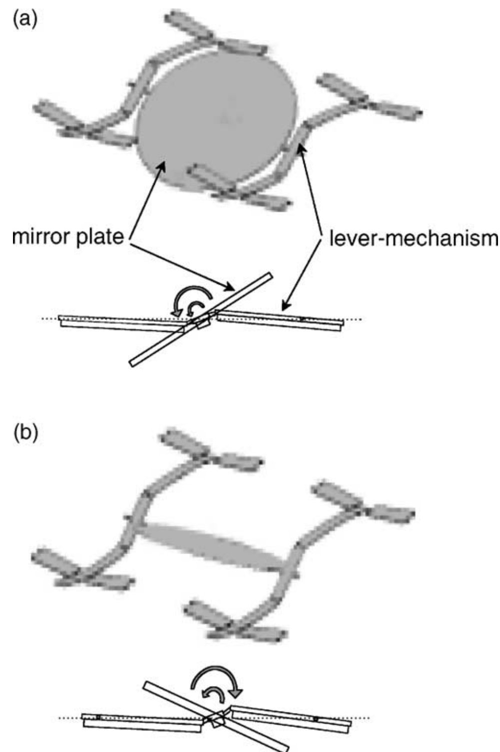

Fig. 6. The mirror plate and couplers vibrate (a) in-phase at the first torsional mode, and (b) out-of-phase at the second torsional mode.

should have three torsional vibration modes. According to the finite element analysis, the angular motions of the coupler and the mirror plate are all in phase for the first torsional vibration mode, as illustrated in Fig. 6a; whereas in second torsional vibration mode the angular motions of the couplers and the mirror plate are out of phase, as illustrated in Fig. 6b. Thus, the higher vibration mode of the scanner can be exploited to meet the requirement of a high scanning frequency.

3. Experiment and results

In order to demonstrate the concept proposed in this study, a micromachining process integrating DRIE, surface micromachining, and bulk wet etch is proposed to realize the micro torsional mirrors shown in Fig. 1. In addition, an experimental setup was established to characterize the flatness and dynamic performance of the torsional mirror.

3.1. Fabrication processes

A highly integrated, monolithic micromachining process was devised in this study. The deep trench etched by ICP and thin-film refilled process could be used to fabricate a stiff and light structure. Surface micromachining provides narrow-gap electrodes and the flexure structure. The bulk anisotropic wet etching undercuts a cavity on the substrate to provide a space for the motions of the mirror plate and

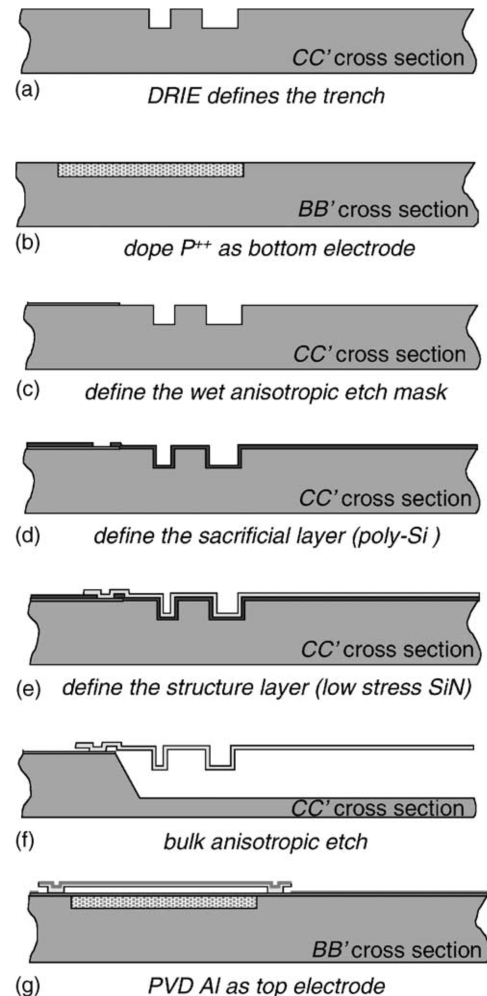

Fig. 7. Fabrication processes (the cross-sections are defined in Fig. 1).

lever mechanism. The three different micromachining depths required are 2, 15, and 200 μm, which can be produced in a monosubstrate using the thin-film structure and sacrificial layer, DRIE trenching, and bulk etching, respectively.

The five masking processes are illustrated in Fig. 7, and the cross-sections indicated in the figure correspond to those shown in Fig. 1a. Firstly, Fig. 7a shows that the Si substrate was DRIE for 15 μm to define the depth *d* of the rib-reinforced lever arms and the folded frame. Fig. 7b shows that a boron-doping process was used to define the bottom electrodes. In addition, the boron concentration of the doped layer was heavy enough to stop the bulk etching. After that, 1000 Å thermal SiO_2 was grown and 2000 Å of LPCVD Si_3N_4 deposited and patterned to define the etching mask for the bulk anisotropic wet etching, as illustrated in Fig. 7c. A 2-μm-thick LPCVD poly-Si was then deposited and patterned as the sacrificial layer, as shown in Fig. 7d; low-temperature (585 °C) fine-grain poly-Si was employed to ensure a smooth surface was produced. In the fifth step, a 2.5-μm-thick LPCVD low-stress SiN layer was deposited and patterned as the structural layer, as shown in Fig. 7e. The substrate was then bulk etched by KOH, which would

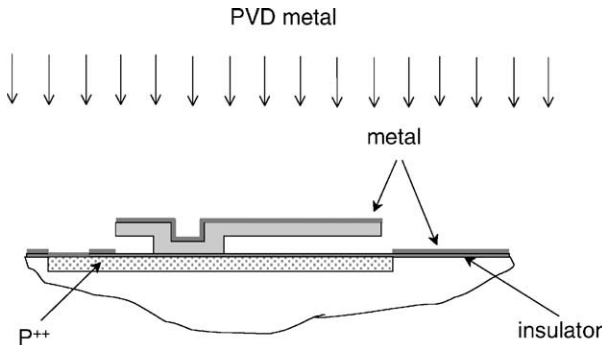

Fig. 8. Self-alignment isolation caused by the shadow effect.

first remove the poly-Si sacrificial layer. The Si substrate that was not protected by the etching mask (as illustrated in Fig. 7c) was etched by the KOH solution after the sacrificial layer had been removed. Finally, the lever mechanisms and the mirror plate of the torsional mirror were suspended (Fig. 7f). The fabrication processes were complete once the top electrodes had been deposited using a physical vapor deposition (PVD, i.e. evaporation or sputtering) Al film, as shown in Fig. 7g.

The shadow effect illustrated in Fig. 8 was exploited to isolate the top electrodes and the substrate during the PVD process. The scanning electron micrographs in Fig. 9 show different views of a typical torsional mirror fabricated using the above processes. The torsional mirror is driven by two torque generators that are located symmetrically at both sides of the mirror plate. The driving electrodes are 100 μm wide and 200 μm long, the lever arm is 600 μm long and 50 μm wide, and the mirror plate is 650 μm in diameter. The size of the cavity etched by the KOH solution can be adjusted by varying the etching time, to allow the mirror plate to rotate out-of-plane freely according to the desired scanning angle.

The above fabrication processes provide four advantages over various existing processes. Firstly, the overall fabrication process successfully integrated the DRIE, surface, and bulk processes; thus the bonding and mold-separation processes needed in the HexSil technique [12] were not required. Secondly, the DRIE process can be used to adjust the stiffness of each component, even when their thicknesses are the same. Thirdly, the size of the cavity etched by the KOH solution can be adjusted by varying the bulk etching time to allow the mirror plate to rotate out-of-plane freely. Fourthly, the top electrode is formed by the PVD Al film after the bulk etching process; hence is was not necessary to protect the Al film during bulk etching.

3.2. Experimental results

An interferometer was used to measure the surface profile of the mirror under static loading conditions. Typical results for mirrors without and with the reinforced frame are shown in Fig. 10a and b, respectively. Fig. 10a shows that the bending radii of the mirror without the reinforced frame

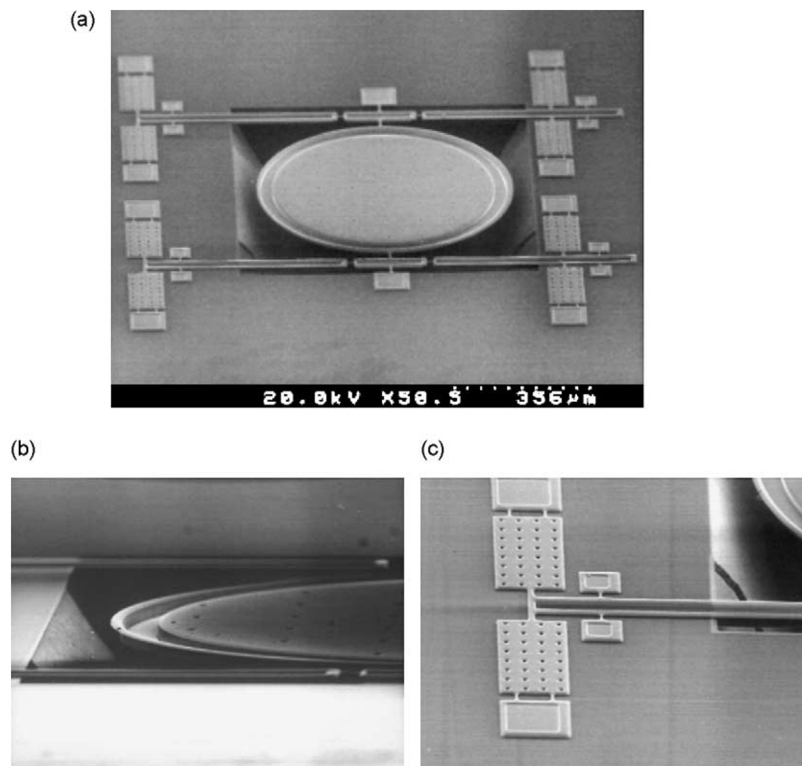

Fig. 9. Scanning electron micrographs showing of (a) the overview of the micro torsional mirror, (b) the close-up of the reinforced frame of the mirror plate, and (c) the close-up of gap-closing electrodes and lever mechanism.

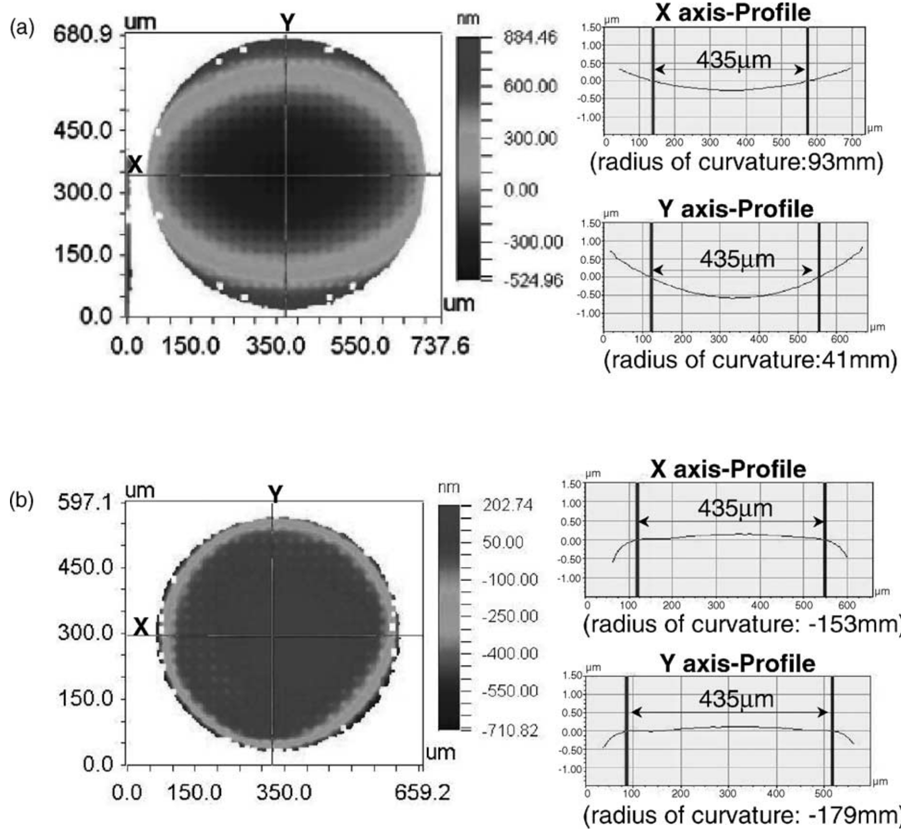

Fig. 10. Measured surface profile of (a) the mirror plate without folded frame, and (b) the mirror plate with folded frame.

are $\rho_x = 9.3$ cm and $\rho_y = 4.1$ cm in the x and y directions, respectively. This difference is attributable to the constraint provided by the torsion bar in the x direction. Fig. 10b shows that the corresponding bending radii of the mirror plate with folded frame ($w = 30\,\mu$m and $d = 15\,\mu$m) were $\rho_x = 15.3$ cm and $\rho_y = 17.9$ cm. The bending of the mirror plate by the static load (gradient residual stress, σ_g) is significantly reduced by the folded frame. In addition, the asymmetry of curvature due to the torsional bar has also been reduced. These results demonstrate that the folded frame not only reduces the bending of the mirror plate but also isolates the constraint loads caused by the torsional suspension.

An experimental setup was established to characterize the dynamic behavior of the torsional mirror. A function generator and power amplifier were used to drive the torsional mirror. A Laser Doppler Vibrometer was used to measure the

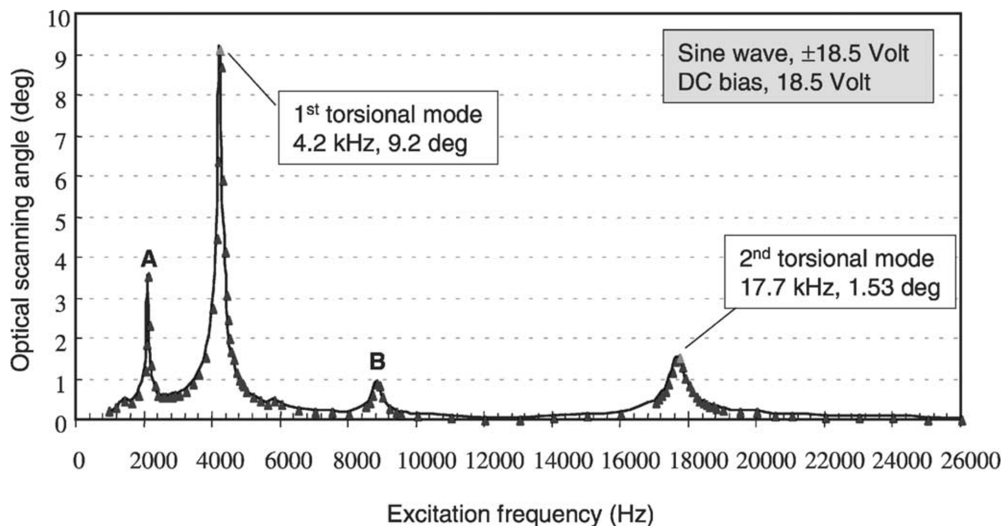

Fig. 11. Frequency response of the proposed micro torsional mirror.

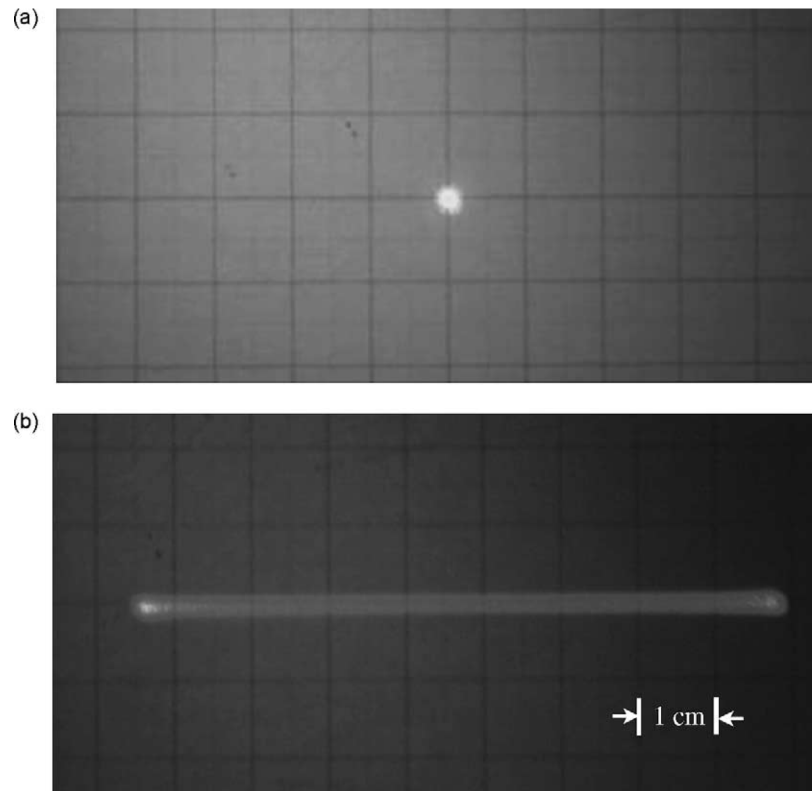

Fig. 12. The laser beam reflected from the micro torsional mirror, (a) when mirror is stationary, and (b) when mirror is driven at its resonant frequency; the distance from the mirror to the image plane was 50 cm.

dynamic characteristics of the mirror plate, in terms of vibration frequencies and amplitudes. The measured frequency response in Fig. 11 shows the variation of the optical scanning angle as a function of the driving frequency of the torsional mirror. The electrodes were driven by a ±18.5-V ac signal V_a with a 18.5-V dc bias V_d. Fig. 11 indicates that the first torsional mode of this scanner occurred at $f_1 = 4.2$ kHz, with a corresponding scanning angle of 9.2°. The second torsional mode of this scanner occurred at $f_2 = 17.7$ kHz, with a corresponding scanning angle of 1.5°. The scanning angle of the second mode increased to 5.0° when the driving voltages became $V_a = \pm 26.5$ V and $V_d = 20.0$ V. Since the driving force is proportional to $[V_d + V_a \sin(\omega t)]^2$, the excitation contains components at both ω and 2ω, and thus the mirror plate will also experience resonant peaks when the driving frequencies are at $f_1/2$ and $f_2/2$ (i.e. 2.1 and 8.85 kHz), respectively. These two additional peaks were evident in the experiment data (marked as "A" and "B" in Fig. 11). A photograph of the reflected laser-beam trace at the first torsional mode is shown in Fig. 12.

4. Discussion and conclusions

There are several metal films that could be used in this device, although the associated metalization processes would differ. For instance, gold could be deposited and patterned before bulk etching, since it would not be attacked by KOH. Al film is also a potential candidate because of its high reflectivity and low residual stress, but Al would have to be deposited after bulk etching since it would be attacked by the KOH. Thus, a shadow mask would be required during the PVD process—as indicated in Fig. 8, the shadow effect is exploited in this study to avoid the need for a shadow mask during the PVD process. The testing results show that the electrodes will not break down when the driving voltage is smaller than 80 V.

In conclusion, a novel micro torsional mirror for use as a high-frequency optical scanner is studied. The micro torsional mirror consists of a driving mechanism and a reinforced mirror plate. The driving mechanism of the torsional mirror contains two narrow-gap electrodes, two levers, and a coupler. This micro torsional mirror exhibits four merits: (1) the driving voltage is lower due to the use of the gap-closing parallel-plate electrodes, and the traveling distance is remarkably magnified by the lever mechanism; (2) the mirror plate is subjected to a pure torque generated by the driving mechanism, thereby preventing wobble motion of the mirror plate; (3) the stiffness and flatness of the mirror plate is increased by incorporating a reinforced frame, which improves the optical performance of the scanner; and (4) the mirror can be used at a higher scanning frequency due to the higher vibration mode of the three-mass system. Micromachined torsional mirrors were fabricated through

the integration of DRIE, surface, and bulk micromachining processes. Interferometric and LDV measurements demonstrated that the mirror exhibited a second vibration mode at 17.7 kHz, with a scan angle of 5°.

Acknowledgements

This material is based (in part) upon work supported by the National Science Council (Taiwan) under Grant NSC 89-2218-E-007-011 and Walsin Lihwa Corp. The author would like to appreciate the National Science Council Central Regional MEMS Research Center, Taiwan; the Electrical Engineering Department of National Tsing Hua University, Taiwan; Semiconductor Center of National Chiao Tung University, Taiwan; and National Nano Device Laboratory, Taiwan in providing the fabrication facilities. The authors would also like to thank Prof. R.-S. Huang for his valuable suggestions.

References

[1] K.E. Peterson, Silicon torsional scanning mirror, IBM J. Res. Dev. 24 (5) (1980) 631–637.

[2] L.J. Hornbeck, Current Status of The Digital Micromirror Device (DMD) for Projection Television Applications, Int. Electron Devices Tech. Dig., Dallas, TX, December 1993, pp. 381–384.

[3] M.-H. Kiang, O. Solgaard, R.S. Muller, K.Y. Lau, Surface-Micromachined Electrostatic-Comb Driven Scanning Micromirrors for Barcode Scanners, IEEE MEMS Workshop, San Diego, CA, February 1996, pp. 192–197.

[4] M.-H. Kiang, O. Solgaard, R.S. Muller, K.Y. Lau, Electrostatic combdrive-actuated micromirrors for laser-beam scanning and positioning, J. Microelectromech. Sys. 7 (1) (1998) 27–37.

[5] P.M. Hagelin, O. Solgaard, Optical raster-scanning displays based on surface-micromachined polysilicon mirrors, IEEE Sel. Topics Quantum Electr. 5 (1) (1999) 67–74.

[6] K.S.J. Pister, M.W. Judy, S.R. Burgett, R.S. Fearing, Microfabricated hinges, Sens. Actuators A 33 (1992) 249–256.

[7] R.A. Conant, P.M. Hagelin, O. Solgaard, K.Y. Lau, R.S. Muller, A Raster-Scanning Full-Motion Video Display Using Polysilicon Micromachined Mirrors, Transducers 1999, Sendai, Japan, June 1999, pp. 376–379.

[8] H.-Y. Lin, W. Fang, Out-of -plane comb-drive lever actuator, ASME IMECE 2000, Orlando, FL, November 2000, pp. 97–103.

[9] H.-Y. Lin, W. Fang, Rib-reinforced micromachined beam and it applications, J. Micromech. Microeng. 10 (2000) 93–99.

[10] J.T. Nee, R.A. Conant, M.R. Hart, R.S. Muller, K.Y. Lau, Stretched-film micromirrors for improved optical flatness, in: Proceedings of the IEEE MEMS'2000, Miyazaki, Japan, January 2000, pp. 704–709.

[11] H.-Y. Lin, W. Fang, The improvement of the micro torsional mirror by a reinforced folded frame, ASME IMECE 2000, Orlando, FL, November 2000, pp. 189–194.

[12] C.G. Keller, R.T. Howe, Nickel-filled Hexsil thermally actuated tweezers, Transducers 1995, Stockholm, Sweden, June 1995, pp. 376–379.

Biographies

Weileun Fang was born in Taipei, Taiwan, in 1962. He received PhD degree from Carnegie Mellon University in 1995. His doctoral research focused on the determining of the mechanical properties of thin films using micromachined structures. In 1995, he worked as a postdoctoral research at Synchrotron Radiation Research Center, Taiwan. He is currently an associate professor at Power Mechanical Engineering Department, National Tsing Hua University, Taiwan. His research interests include MEMS with emphasis on micro optical systems, microactuators and the characterization of the mechanical properties of thin films.

Hung-Yi Lin was born in Taiwan, in 1974. He received the MS and PhD degrees in mechanical engineering from National Tsing Hua University, Hsinchu, Taiwan, in 1998 and 2002, respectively. He is working at the R&D department of Walsin Lihwa Corp., Taiwan, as a project leader. His research interests are the development of novel MEMS fabrication platform and micro optical systems.